



ELSEVIER

Physica D 100 (1997) 279–300

PHYSICA D

Self-synchronization of coupled oscillators with hysteretic responses

Hisaki Tanaka^{a,b,*}, Allan J. Lichtenberg^b, Shin'ichi Oishi^a^a *Department of Information and Computer Sciences, Waseda University, Tokyo 169, Japan*^b *Electronics Research Laboratory and Department of Electrical Engineering and Computer Sciences, University of California, Berkeley, CA 94720, USA*

Received 21 May 1996; revised 26 July 1996; accepted 26 July 1996

Communicated by Y. Kuramoto

Abstract

We analyze a large system of nonlinear phase oscillators with sinusoidal nonlinearity, uniformly distributed natural frequencies and global all-to-all coupling, which is an extension of Kuramoto's model to second-order systems. For small coupling, the system evolves to an incoherent state with the phases of all the oscillators distributed uniformly. As the coupling is increased, the system exhibits a discontinuous transition to the coherently synchronized state at a pinning threshold of the coupling strength, or to a partially synchronized oscillation coherent state at a certain threshold below the pinning threshold. If the coupling is decreased from a strong coupling with all the oscillators synchronized coherently, this coherence can persist until the depinning threshold which is less than the pinning threshold, resulting in hysteretic synchrony depending on the initial configuration of the oscillators. We obtain analytically both the pinning and depinning threshold and also explain the discontinuous transition at the thresholds for the underdamped case in the large system size limit. Numerical exploration shows the oscillatory partially coherent state bifurcates at the depinning threshold and also suggests that this state persists independent of the system size. The system studied here provides a simple model for collective behaviour in damped driven high-dimensional Hamiltonian systems which can explain the synchronous firing of certain fireflies or neural oscillators with frequency adaptation and may also be applicable to interconnected power systems.

PACS: 02.50.-r; 05.40.+j; 05.90.+m; 84.30.Jc; 87.10.+e

Keywords: Phase model; Mutual entrainment; Hysteresis; Bifurcation; Adaption

1. Introduction

There has been a continuing effort to understand the collective synchronous behaviour in dynamical systems with many degrees of freedom. Particularly, for the spontaneous emergence of synchronization, extensive studies have been devoted to large populations of limit-cycle oscillators ([1–3,5,6,15,16,20–24,26,29–31,38], see [27] for many other interesting references). The studies have been motivated by intrinsic scientific interest [4,8,9,12,13,17,36,37] along with the applications to engineering [7,11,13,32,33,35,39]. Recently, a breakthrough has been made in [35]

* Corresponding author. E-mail: tanaka@oishi.info.waseda.ac.jp.

that relates the study of a practical current-biased series array of non-identical Josephson junctions and Kuramoto's theory on spontaneous synchrony which was originally a product of an ingenious and bold insight in nonlinear physics [15,16,24].

Certain interacting limit-cycle oscillators can be reduced to a *phase model* through averaging, allowing them to be approximated by a set of first-order phase equations of the form

$$\frac{d\theta_i}{dt} = \omega_i + \sum_j H_{ji}(\theta_j - \theta_i), \quad (1)$$

in order to analyze their synchrony. On the other hand, systems with many degrees of freedom of the form

$$\frac{d^2\theta_i}{dt^2} = \sum_j H_{ji}(\theta_j - \theta_i) \quad (2)$$

can be Hamiltonian, having special dynamical characteristics [14,19,34]. A damped, driven generalization of (1) and (2)

$$m \frac{d^2\theta_i}{dt^2} + \frac{d\theta_i}{dt} = \Omega_i + \sum_j H_{ji}(\theta_j - \theta_i) \quad (3)$$

is a practical model for systems with many degrees of freedom in various fields of science. The question naturally arises to the behavior of (3): do the oscillators synchronize as in (1) or do they exhibit dynamical patterns which are a remnant of the dynamics in (2)?

Another motivation of this work is related to the progress in modeling the synchronous firing of the southeast Asia fireflies – *Pteroptyx malaccaae*. Unlike other species such as *P. cribellata*, *P. malaccaae* has an ability to alter its firing frequency as much as 15% to higher or lower frequency in response to the external signals, and this adaptation is considered to be responsible for the synchronous firing with very small phase lags [12]. Based on the physiological reasoning as well as the data from field work by Hanson [12], Ermentrout [8] developed a phase model explaining the synchronous firing in swarms of *P. malaccaae*. His idea is to introduce an adaptive effect of the firing frequency to the phase model (1), as the simplest model for synchronous firing with small phase lags, in the following way:

$$\dot{\theta}_i = \omega_i, \quad \dot{\omega}_i = \epsilon(\omega_{i0} - \omega_i) + \sum_{j=1}^N H_{ji}(\theta_j - \theta_i). \quad (4)$$

Choosing small ϵ and a particular function H_{ji} (which can be nearly sinusoidal if ω_i is in the range of adaptive frequency), phase model (4) can simulate the synchrony observed in swarms of *P. malaccaae* [8]. Interestingly, (4) is equivalent to (3) if (3) has an all-to-all, global coupling. More specifically, (4) can be transformed to

$$m\ddot{\theta}_i + \dot{\theta}_i = \Omega_i + (K/N) \sum_{j=1}^N h(\theta_j - \theta_i), \quad i = 1, \dots, N \quad (5)$$

by assuming that all H_{ji} are identical and letting

$$t_{\text{old}} \rightarrow \epsilon t_{\text{new}}, \quad \Omega_i = \epsilon \omega_{i0}, \quad H_{ji}(\theta_j - \theta_i) = (K/N)h(\theta_j - \theta_i), \quad m = \epsilon^{-2}. \quad (6)$$

Here, we study the particular model (5) with sinusoidal nonlinearity $h(\cdot) = \sin(\cdot)$. In addition to the interest in firefly synchrony, this model may be significant for understanding the synchrony in power systems modeled by the swing equation [25], and also to extend the analysis of the Hamiltonian system studied by Konishi and Kaneko [14] to a damped, driven (continuous time) system.

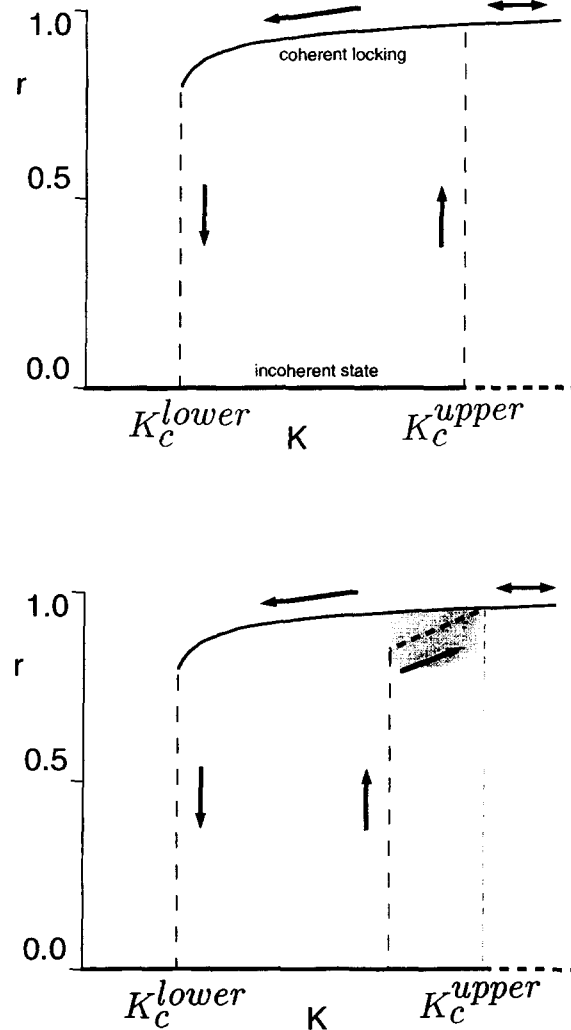


Fig. 1. Hysteretic synchrony observed in (5) with system size $N = 500$. (a) As K exceeds the depinning threshold K_D the system switches discontinuously from the incoherent state to the coherent locked state. The data were obtained for $m \sim 0.85$ and uniformly distributed Ω_i in $[-5.0, 5.0]$. (b) For larger m (~ 0.95) and the same natural frequency distribution Ω_M as in (a), the system exhibits an oscillation of the coherence r in the shaded region. The dotted line shows a time average of r .

In this paper, we consider the phase model (5) to understand the effect of inertia, namely frequency adaptation to synchrony of oscillators. The main new finding is that the system can exhibit *hysteretic synchrony* depending on the initial conditions. A schematic illustration of this phenomenon is shown in Figs. 1(a) and (b). The vertical axis represents a degree of the synchrony of the oscillators which will be explicitly defined in Section 2. Fig. 1(a) shows the simplest pattern obtained numerically for $m = 0.75$, $\Omega_M = 5.0$ and $N = 500$ where the hysteresis is characterized by two different sets of (K, r) values at which a discontinuous jump across between the incoherent state and coherent synchronized state. This kind of hysteretic synchrony has been observed in the charged density wave (CDW) model studied in [29]. While in Fig. 1(b), an oscillation of the coherence r can be observed in the shaded region for $m = 0.85$ and the other conditions as in Fig. 1(a), it suggests, that the synchrony in (5) has a more involved nature than in the CDW model [29]. The common feature observed in Figs. 1(a) and (b) can be

summarized as follows: (i) there is an upper/lower limit of K where the coherent synchrony onsets/disappears; and (ii) the coherent synchronized state and the incoherent state can coexist for a certain coupling strength K between the upper and lower limits of K .

This paper aims to clarify these characteristics in the limit of large N and to examine the oscillating state of the coherence. The paper is organized as follows. In Section 2, to make our starting point clear, we review the self-consistent theory of Kuramoto's model in its simplest form. In Section 3, we develop a self-consistent theory for the synchrony of (5) in the limit of $N \rightarrow \infty$. The main idea is an extension of Kuramoto's theory which involves the self-consistent mean field theory taking different initial configurations of oscillations into account. In Section 3.1, we introduce an order parameter r to decouple (5) into a swarm of single pendulum oscillators and consider the hysteretic response of each oscillator. In Section 3.2, we start from a system with a distribution of the natural frequencies Ω_M , for which two different self-consistent equations are derived, corresponding to the two different initial configurations of oscillators. We then focus on one simplifying case in Section 3.3, that permits an analytical treatment of the self-consistent equation – that of uniformly distributed natural frequencies in a finite range $[-\Omega_M, \Omega_M]$ and $m \cdot K \gg 1$. From the self-consistent equation, which is perturbatively approximated under these conditions, analytic results are obtained in Section 3.4, i.e. the lower and upper critical points and the associated discontinuous jumping between incoherent and coherent synchronized states are obtained. Specifically, the lower critical point is shown to be the same as that from the original Kuramoto model, while the upper critical point is obtained from a set of nonlinear finite-dimensional equations and shown to have a greater K than the lower critical point.

In the numerical part (Section 4), we numerically simulate the model (5), and verify the existence of hysteretic synchrony, where the lower and upper critical points are obtained and show a nice agreement with the theoretical prediction in Section 3.4. In addition to the hysteretic synchrony phenomena, we examine the oscillatory state of the coherence r for different system size N and coupling strength K to explore the size dependence of the oscillatory region.

2. Kuramoto's theory in its simplest form

The “phase transition”-like synchronization onset is a large population of interacting oscillators and was first described by Winfree in [36]. An analytically tractable model, the Kuramoto model, was then proposed by Kuramoto to elucidate a subtle connection between collective synchronization and phase transitions [15,16,24]. The Kuramoto model, which is derived by averaging from a certain class of weakly, globally coupled limit-cycle oscillators, takes the following form in the simplest case:

$$\dot{\theta}_i = \Omega_i + (K/N) \sum_{j=1}^N \sin(\theta_j - \theta_i), \quad i = 1, \dots, N. \quad (7)$$

Here, θ_i and Ω_i are respectively, the instantaneous phase and the natural frequency of the i th oscillator, and $K/N \geq 0$ is the coupling strength. In the large N limit, we assume that the intrinsic frequencies have a certain distribution $g(\Omega)$. Since (7) has the arbitrariness in shifting all θ_i by Ω_i , we can assume the distribution $g(\Omega)$ becomes zero-mean after a shift. Here, we consider a unimodal, symmetric distribution $g(\Omega)$ with $g(\Omega) = g(-\Omega)$ which includes the Gaussian and also the uniform distribution, although certain bimodal distributions can be considered as in [16]. The “all-to-all” global coupling in (7) might seem unrealistic at the first sight, but this global coupling arises naturally in certain circumstances; for example, in realistic, electrical systems such as a Josephson array [35] and the interaction of quasi-optical oscillators with a cavity [39]. The uniform global coupling in (7) provides a simplifying property

that enables one to utilize the “mean field” description of macroscopic behavior. This can be realized by use of “order parameters” r and ϕ defined by

$$r e^{i\phi} = (1/N) \sum_{j=1}^N e^{i\theta_j} \tag{8}$$

in which $r = r(t)$ and $\phi = \phi(t)$ can be interpreted as the degree of synchrony and the mean phase angle, respectively. From a trigonometric identity and (8), one can transform (7) equivalently to the following set of equations:

$$\dot{\theta}_i = \Omega_i + K r \sin(\phi - \theta_i), \quad i = 1, \dots, N. \tag{9}$$

In (9), each oscillator is equivalent to an overdamped pendulum with torque Ω_i and restoring force proportional to Kr . Thus, the order parameters r and ϕ determine the time evolution of θ_i , and θ_i determines r and ϕ self-consistently by (8). Using the above formalism, Kuramoto obtained the following key insight:

[A1] There are self-consistent steady solutions of (8) and (9). In particular, there are solutions with $r(t)$ and $\phi(t)$ being constant, in which all fluctuations vanish in the large N limit.

In the present situation, ϕ can be set to 0 without loss of generality from the arbitrariness of θ_i in (7). One “trivial” solution is found to be $r(t) \equiv 0$, where all oscillators rotate at their intrinsic frequencies. This completely incoherent solution exists for all K , but is not necessarily stable. A secondary family of steady solutions bifurcates at $K = K_c$ with

$$K_c = \frac{2}{\pi g(0)}. \tag{10}$$

This critical value can be obtained from the self-consistent formalism which is briefly explained as follows. For a given $g(\Omega)$ and constraints $K \geq K_c$ and $r > 0$, the oscillators are separated into two groups. One group is the mutually synchronized oscillators with $|\Omega| \leq Kr$ (denoted by [S]), and the other group is the drifting oscillators with $|\Omega| > Kr$ (denoted by [D]). In the synchronized group [S], each oscillator is locked to the mean phase with phase lags determined by (9). A drifting oscillator in [D] with a natural frequency Ω has a velocity $\dot{\theta}$ also determined by (9). Thus, given the natural frequency distribution $g(\Omega)$, the normalized density of the oscillators in [S] and [D] can be, respectively, obtained explicitly as $n_S(\theta)$ and $n_D(\theta, \Omega)$ through [15,16,24]. This static density of oscillators on the unit circle of $\theta \in [0, 2\pi)$ determines the contribution to the mean phase from the oscillators in [S] and [D]. Namely, the contribution of the locked oscillators [S] is expressed as

$$r_{\text{lock}} = \oint n_S(\theta) e^{i\theta} d\theta = Kr \int_{-\pi/2}^{\pi/2} \cos^2 \theta g(Kr \sin \theta) d\theta, \tag{11}$$

while the contribution from the drifting oscillators [D] is expressed as

$$r_{\text{drift}} = \oint \int_{|\Omega| > Kr} e^{i\theta} n_D(\theta, \Omega) g(\Omega) d\Omega d\theta = 0. \tag{12}$$

This particular form of r_{lock} appears again for (5) as shown in Section 3.2. The sum of r_{lock} and r_{drift} again determines the mean phase such that the following self-consistent equation must be satisfied [15,16,24]:

$$r = r_{\text{lock}} + r_{\text{drift}}. \tag{13}$$

We see in (12) that r_{drift} vanishes due to the symmetry of $g(\Omega)$, $g(\Omega) = g(-\Omega)$, i.e. in the Kuramoto model with symmetric $g(\Omega)$, a swarm of evenly distributed oscillators has no effect on r . However, this cancellation does not

hold for (5), even for a symmetric $g(\Omega)$, as we see in Section 3. Thus, assuming $Kr \sin \theta$ is small in $g(\cdot)$ of (11), we are led to the following equation from (13):

$$r = r_{\text{lock}} + r_{\text{drift}} = r_{\text{lock}} \simeq \frac{1}{2}\pi Kr g(0) - \frac{1}{16}\pi K^3 r^3 g^{(2)}(0) + O(r^4). \quad (14)$$

Dividing (14) by r and letting $r \rightarrow 0$, we find $K_c = 2/\pi g(0)$ and the coherence factor r grows as $(K - K_c)^{1/2}$ just above the transition at $K = K_c$. The exponent $\frac{1}{2}$ is due to the pure sine nonlinearity in (7) [6], and thus shows the analogy to the second-order phase transition in magnetic spins. It should be mentioned that much progress has been made in this formalism; see for example [24] for modulated sinusoidal coupling function, and [6] for certain general periodic functions.

3. Extension of Kuramoto's theory to a second-order system

In this section, we develop a self-consistent theory for the coherence r in (5) (hereafter, we call (5) the extended Kuramoto model). The basic idea is the same as Kuramoto's, however, the analysis for the extended Kuramoto model becomes more involved because (a) Eq. (5) is generalized from a second-order system (a pendulum equation) whose static states can be multi-stable and, therefore, dependent on the initial conditions, and (b) there is no longer an exact solution to (5) for the drifting oscillators. We start from general m , K and $g(\Omega)$ with $g(\Omega) = g(-\Omega)$, and derive self-consistent for different configurations of initial conditions taking the above property (a) into account, then focus on one simplifying case of m , K and $g(\Omega)$ which enables us to give a good approximation of the solution and the density of drifting oscillators on the unit circle.

3.1. Governing equation and hysteretic curve of $(\Omega, \langle \dot{\theta} \rangle)$

Utilizing the identity $(K/N) \sum_{j=1}^N \sin(\theta_j - \theta_i) = Kr \sin(\phi - \theta_i)$ as obtained from (8) and a trigonometric identity, (5) can be transformed to

$$m\ddot{\theta}_i + \dot{\theta}_i = \Omega_i - Kr \sin \theta_i, \quad i = 1, \dots, N, \quad (15)$$

which is the governing equation for a single damped driven pendulum. A damped driven pendulum is known to have hysteresis with respect to the initial conditions $(\theta_i, \dot{\theta}_i)$, which can be characterized by two different driving frequencies: the pinning frequency Ω_P and the depinning frequency Ω_D . As shown in Fig. 2, a pendulum starts whirling once the applied torque Ω goes beyond a certain threshold Ω_D . This Ω_D is characterized by the disappearance of the equilibrium point determined by (15): $\theta = \sin^{-1}(\Omega/Kr) = \pm \frac{1}{2}\pi$. Then $\Omega_D (> 0)$ is given by $\Omega_D = Kr$. On the other hand, once a pendulum starts whirling, it continues to rotate even though the torque Ω is varied down below Ω_D . This is due to the inertia of the pendulum and can be understood by the appearance of the second kind of periodic solution in a two-dimensional phase portrait of (15) which is well understood (for example, see [18]).

If Ω is again brought down, the frequency of $\tilde{\Omega} \equiv \langle \dot{\theta} \rangle$ which is the average of $\dot{\theta}$ over one period, tends to 0 continuously as Ω_P is approached. Specifically, if the damping is sufficiently small (underdamped case), $\langle \dot{\theta} \rangle$ tends to 0 as $[\ln(\Omega - \Omega_P)]^{-1}$, which means the falling of the frequency of the running periodic solution θ , becomes extremely steep as Ω tends to Ω_P [28]. Furthermore, in this underdamped case an analytical approximation of Ω_P becomes possible, using Melnikov's method [10] (see Appendix B for the derivation of Ω_P).

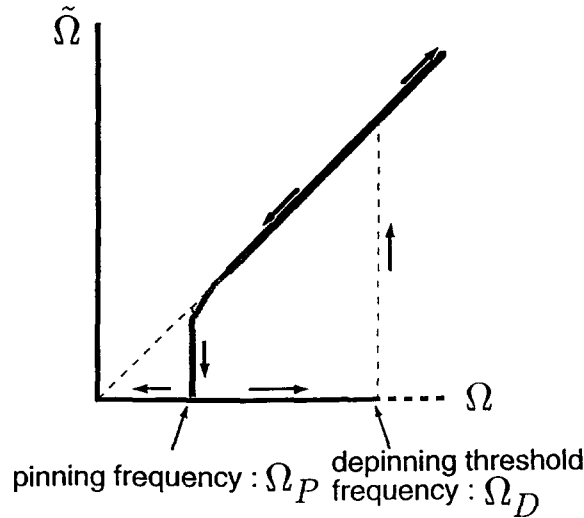


Fig. 2. $(\Omega, \langle \theta \rangle)$ curve for a single oscillator.

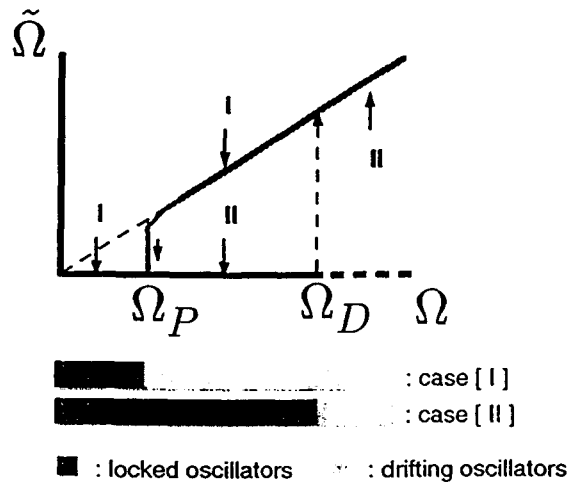


Fig. 3. Locked oscillators [S] and drifting oscillators [D] distributed on $(\Omega, \langle \theta \rangle)$ curve.

3.2. Self-consistent equation for two different cases

We now look for a solution of (15) satisfying [A1] by deriving a self-consistent equation determining the coherence r . There are two cases to be considered: case [I] in which the coupling strength K is increased from the incoherent $r = 0$ state; and the case [II] in which K is decreased from the coherent state with $r \simeq 1$. In both cases, we start by assuming the state where there are swarms of locked and drifting oscillators and they have some coherence r_{lock} and r_{drift} , respectively. In case [I], suppose a certain r is given at any moment, then r determines the pinning threshold Ω_P and the initially drifting oscillators with $\Omega < \Omega_P$ can be entertained to the locked oscillators [S] after a certain transient. Thus, it is reasonable to assume that the swarms of [S] and the drifting oscillators [D] can be separated at $\Omega = \Omega_P$ in the natural frequency distribution as shown in Fig. 3. On the other hand, in case [II] initially locked

oscillators are desynchronized and fall into the drifting state [D] once Ω exceeds $\Omega_D (= Kr)$. Hence, [S] and [D] can be assumed to be separated at the depinning frequency $\Omega = \Omega_D$.

The coherence r_{lock} for case [II] takes exactly the same form as (11) in Kuramoto’s theory:

$$r_{\text{lock}}^{\text{II}} = \oint n_S(\theta)e^{i\theta} d\theta = \int_{|\Omega| < \Omega_D} g(\Omega)e^{i\theta} d\Omega = Kr \int_{-\pi/2}^{\pi/2} \cos^2 \theta g(Kr \sin \theta) d\theta, \tag{16}$$

where n_S is the normalized density of the synchronized oscillators with phase θ . In (16), the relations $n_S(\theta) = g(\Omega) d\Omega/d\theta$ and $Kr \cos \theta = d\Omega/d\theta$ were used. For case [I], oscillators with $\Omega > \Omega_P$ are still drifting on the unit circle and the coherence of the locked oscillators takes the following form:

$$\begin{aligned} r_{\text{lock}}^{\text{I}} &= \oint n_S(\theta)e^{i\theta} d\theta = \int_{|\Omega| < \Omega_P} g(\Omega)e^{i\theta} d\Omega = \int_{-\sin^{-1}[\Omega_P/(Kr)]}^{\sin^{-1}[\Omega_P/(Kr)]} e^{i\theta} g(Kr \sin \theta) K \cos \theta d\theta \\ &= Kr \int_{-\theta_P}^{\theta_P} \cos^2 \theta g(Kr \sin \theta) d\theta, \end{aligned} \tag{17}$$

where $\theta_P = \sin^{-1} \Omega_P/(Kr)$ and $\theta_P < \frac{1}{2}\pi$ follows from $\Omega_P < \Omega_D = Kr$.

Now we consider the effect from [D] on r :

$$r_{\text{drift}}^{1,\text{II}} = \int_{|\Omega| > \Omega_{P,D}} \oint e^{i\theta} n_D(\theta, \Omega) g(\Omega) d\theta d\Omega, \tag{18}$$

where $n_D(\theta, \Omega)$ is the density of the desynchronized oscillators [D] with phase θ and given by driving frequency Ω . As $n_D(\theta, \Omega)$ is proportional to $|\dot{\theta}|^{-1}$ and $\oint n_D(\theta, \Omega) d\theta = \int_0^{\tilde{T}} n_D(\theta, \Omega) \dot{\theta} dt = 1$, we obtain

$$n_D(\theta, \Omega) = \tilde{T}^{-1} |\dot{\theta}|^{-1} = (\tilde{\Omega}/2\pi) |\dot{\theta}|^{-1}. \tag{19}$$

with \tilde{T} and $\tilde{\Omega}$ being the period and the frequency of the running periodic solution of θ , respectively. Thus, $r_{\text{drift}}^{1,\text{II}}$ are, respectively,

$$r_{\text{drift}}^{1,\text{II}} = \int_{|\Omega| > \Omega_{P,D}} \int_0^{\tilde{T}} e^{i\theta(t,\Omega)} (\tilde{\Omega}/2\pi) |\dot{\theta}|^{-1} \dot{\theta} g(\Omega) dt d\Omega = \frac{1}{2\pi} \int_{|\Omega| > \Omega_{P,D}} \int_0^{\tilde{T}} e^{i\theta(t,\Omega)} |\tilde{\Omega}| g(\Omega) dt d\Omega. \tag{20}$$

Here $\theta(t, \Omega)$ denotes the running solution of (15) with driving frequency Ω , and the following properties were used: $\dot{\theta} > 0$ for $\Omega > 0$, $\dot{\theta} < 0$ for $\Omega < 0$, and $\tilde{\Omega}(-\Omega) = -\tilde{\Omega}(\Omega)$. In (20), $\cos \theta(t)$ and $\sin \theta(t)$ are periodic in t because $\theta(t + \tilde{T}) \equiv \theta(t) + 2\pi, \forall t$. Then, the integration of $\cos \theta(t)$ and $\sin \theta(t)$ over one period \tilde{T} does not depend on the span over which the integration is made. Hence, we may assume that $\theta(0, \Omega) = 0$ without loss of generality. Also from (15) and the above initial condition $\theta(0, \Omega) = 0$, we have $m(-\dot{\theta}(t, \Omega)) + (-\dot{\theta}(t, \Omega)) = -\Omega - Kr \sin(-\theta(t, \Omega))$ such that

$$\theta(t, -\Omega) = -\theta(t, \Omega). \tag{21}$$

From $g(\Omega) = g(-\Omega)$, (20) takes the following form:

$$\begin{aligned}
r_{\text{drift}}^{I,II} &= \frac{1}{2\pi} \int_{\Omega > \Omega_{P,D}} \int_0^{\tilde{T}} [\cos \theta(t, \Omega) + \cos \theta(t, -\Omega)] |\tilde{\Omega}| g(\Omega) dt d\Omega \\
&\quad + \frac{1}{2\pi} \int_{\Omega > \Omega_{P,D}} \int_0^{\tilde{T}} [\sin \theta(t, \Omega) + \sin \theta(t, -\Omega)] |\tilde{\Omega}| g(\Omega) dt d\Omega
\end{aligned} \tag{22}$$

and can be simplified by (21) to

$$r_{\text{drift}}^{I,II} = \frac{1}{\pi} \int_{\Omega > \Omega_{P,D}} \int_0^{\tilde{T}} \cos \theta(t, \Omega) |\tilde{\Omega}| g(\Omega) dt d\Omega. \tag{23}$$

Thus, the two self-consistent equations for $r^{I,II}$,

$$r^{I,II} = r_{\text{lock}}^{I,II} + r_{\text{drift}}^{I,II}, \tag{24}$$

are obtained from (16), (17) and (23).

3.3. Perturbation approximation of self-consistent equations

In this section we consider a condition that enables us to treat (24) analytically. For this purpose, the integration in (23) is performed perturbatively. One way to do this without making the inertia term $m\ddot{\theta}$ small is to start from the underdamped case of (15) with uniform distribution of natural frequency Ω . We consider this in detail below.

First, in a new time-scale: $t_{\text{old}} = mt_{\text{new}}$, (15) takes the form

$$\ddot{\theta}_i + \dot{\theta}_i = m\Omega_i - mKr \sin \theta_i, = m' \left(\frac{m}{m'} \Omega_i \right) - m' \left(\frac{m}{m'} K \right) r \sin \theta_i. \tag{25}$$

This implies that the original (15) with given m is equivalent to a new system with arbitrary m' and an associated rescaled distribution of Ω_i , together with the rescaled K . For instance, suppose that we have a coherence r for (15), with $m = 1.0$, uniformly distributed $\Omega \in [-\Omega_M, \Omega_M]$ with $\Omega_M = 5.0$ and $K = 10.0$, then the same r will be obtained for $m = 0.1$, $\Omega_M = 50.0$ and $K = 100.0$. Thus we do not have to consider m and Ω_M/K separately and we are naturally led to one possible way to introduce a small parameter δ in the underdamped (15): $\delta \equiv (Km)^{-1} \ll 1$.

By letting $t_{\text{old}} \rightarrow K^{-1}t_{\text{new}}$ and $r = \delta\tilde{r}$ with \tilde{r} being an arbitrary constant, (15) can be transformed to

$$\ddot{\theta} + \delta\dot{\theta} + \delta^2\tilde{r} \sin \theta = \delta\Omega/K. \tag{26}$$

In the underdamped Josephson junction array, the exactly equivalent perturbation equation is used for a single junction equation [32]. The *running* periodic solution in (26) is proved to be unique and globally exponentially stable [18]. We look for a series expression of this running periodic solution $\theta(t)$ using the Poincaré–Lindstead method as follows. First, by setting

$$\theta(\tilde{\Omega}t) = \theta_0(\tilde{\Omega}t) + \delta\theta_1(\tilde{\Omega}t) + \dots, \tag{27}$$

$$\tilde{\Omega} = \Omega_0 + \delta\Omega_1 + \dots \tag{28}$$

with period $\tilde{T} = 2\pi/\tilde{\Omega}$ and the initial condition $\theta(0) = 0$, we can obtain the following by matching terms at each power of δ :

$$\begin{aligned} \theta(t) = & \tilde{\Omega}t + \Delta^2\tilde{r} \sin \tilde{\Omega}t + \Delta^3\tilde{r}(\cos \tilde{\Omega}t - 1) + \Delta^4\frac{1}{8}\tilde{r}^2 \sin 2\tilde{\Omega}t - \Delta^4\tilde{r} \sin \tilde{\Omega}t \\ & + \frac{3}{16}\Delta^5\tilde{r}^2(\cos 2\tilde{\Omega}t - 1) - \Delta^5(\tilde{r} + \tilde{r}^2)(\cos \tilde{\Omega}t - 1) + \dots \end{aligned} \tag{29}$$

with $\Delta \equiv (m\Omega)^{-1}$ and $\tilde{r} \equiv \delta^{-1}r = Kmr$, and

$$\tilde{\Omega} = \Omega/K - \frac{1}{2}\tilde{r}^2\Delta^3\delta + \frac{1}{2}\tilde{r}^3\Delta^5\delta - \dots \tag{30}$$

In the above, Ω_n ($n \geq 1$) first becomes non-zero at the term δ^4 term due to the cancellation of the secular term.

Using Ω_p obtained by the Melnikov method (see Appendix B), the following estimates are obtained, which will be used later in this section:

$$\Delta = (m\Omega)^{-1} \leq (m\Omega_p)^{-1} = \frac{1}{4}\pi\sqrt{\delta/r} \tag{31}$$

and

$$\Delta^2\tilde{r} = \Delta r(K/\Omega) \leq (\frac{1}{4}\pi)^2 \sim 0.62. \tag{32}$$

As we shall see in Sections 3.4 and 4, the coherence r takes a value, $\geq \frac{1}{4}\pi$ as shown in Section 3.4, above critical K . This implies that we do not have to consider small r . Thus, we only consider $\delta = (Km)^{-1}$ that satisfies $\delta \ll r$ and $\Delta \ll 1$ from (31). From the series solution of $\theta(t)$ in (29), it can be verified that the coefficients of sin/cos terms are multiplied by $O(\Delta^2\tilde{r})$ as the harmonics increased by one. This multiple $\Delta^2\tilde{r}$ is estimated as $\Delta^2\tilde{r} \leq (\frac{1}{4}\pi)^2$ even at $\Omega = \Omega_p$ as in (32) and this can be much smaller for Ω within $\Omega_p < \Omega < \Omega_M$. Also in (30), the second term, $-(\tilde{r}/2)\Delta^3\delta$, can be estimated from (31) and (32) as $\frac{1}{2}\tilde{r}^2\Delta^3\delta = \frac{1}{2}(\frac{1}{4}\pi)^3r^{1/2}\delta^{1/2} \ll 1$, and the multiplication by $\Delta^2\tilde{r}$ between the higher-order sin/cos terms is verified as in (29). Thus, in the underdamped (26) with $\Delta \ll 1$, the lowest-order (harmonic) solution can be considered to be a reasonable approximation to the *running* periodic solution $\theta(t)$.

Under these conditions, we are now able to derive an analytic approximation of $r_{\text{drift}}^{I,II}$ as follows. By discarding higher-order terms with Δ^n coefficients ($n \geq 4$) in (29), a straightforward calculation (see Appendix A) leads to the integration

$$\int_0^{\tilde{T}} \cos \theta dt \simeq -2(\pi/\tilde{\Omega})J_1(a) \cos(C + \Delta^3\tilde{r}), \tag{33}$$

in which $a = \Delta^2\sqrt{1 + \Delta^2} \cdot \tilde{r}$ and $C = \sin^{-1}(1/\sqrt{1 + \Delta^2})$. From (31) the oscillation amplitude a can be estimated as $a = \Delta^2\sqrt{1 + \Delta^2} \cdot \tilde{r} \leq (\frac{1}{4}\pi)^2\sqrt{1 + (\pi/4)^2(\delta/r)}$. It should be noted that a becomes much smaller than $(\frac{1}{4}\pi)^2$ for $\Omega > \Omega_p$. Hence, $J_1(a)$ in (33) can be approximated as $J_1(a) \simeq \frac{1}{2}a = \Delta^2\sqrt{1 + \Delta^2} \cdot \tilde{r}/2$. Moreover, from $\Delta \leq (m\Omega_p)^{-1}$ and the above approximation, we have to lowest order

$$J_1(a) \cos(C + \Delta^3\tilde{r}) \simeq \frac{1}{2}\tilde{r}\Delta^3 \tag{34}$$

(see Appendix A.) We use (34) to approximate (23) and finally obtain the following:

$$r_{\text{drift}}^{I,II} = \frac{1}{\pi} \int_{\Omega_{p,D}}^{\Omega_M} -2(\pi/\tilde{\Omega})(\tilde{r}/2)\Delta^3|\tilde{\Omega}|g(\Omega) d\Omega = -\frac{Kr}{2\Omega_M} \left[-\frac{1}{2}\Delta^2 \right]_{\Omega_{p,D}}^{\Omega_M}. \tag{35}$$

On the other hand, the uniform distribution of the natural frequency $g(\Omega)$ on $[-\Omega_M, \Omega_M]$ is independent of Ω and therefore gives

$$g(\Omega) = 1/2\Omega_M \quad \text{for } \Omega \in [-\Omega_M, \Omega_M], \tag{36}$$

which reduces (16) and (17), respectively, to the following forms (37) and (38):

$$r_{\text{lock}}^I = Kr \int_{-\theta_p}^{\theta_p} \cos^2 \theta g(Kr \sin \theta) d\theta = \frac{Kr}{2\Omega_M} (\theta_p + \frac{1}{2} \sin 2\theta_p), \tag{37}$$

$$r_{\text{lock}}^{II} = Kr \int_{-\pi/2}^{\pi/2} \cos^2 \theta g(Kr \sin \theta) d\theta = \frac{\pi}{2} \frac{Kr}{2\Omega_M}, \tag{38}$$

where $\theta_p \equiv \sin^{-1}[\Omega_p/(Kr)]$ and $g(Kr \sin \theta) = 1/2\Omega_M$ is used.

For this particular uniform $g(\Omega)$ case, $g(\Omega)$ has a bounded support $[-\Omega_M, \Omega_M]$ and in the cases of $K > K_c^{\text{upper}}$ (in increasing K) and $K > K_c^{\text{lower}}$ (in decreasing K) the contribution from the locked oscillators r_{lock}^M takes the form of $Kr \int_{-\theta_M}^{\theta_M} \cos^2 \theta g(Kr \sin \theta) d\theta$ with $\sin^{-1}[\Omega_M/(Kr)]$.

We note that in Kuramoto’s model with uniformly distributed natural frequencies, the r_{lock} term in (11) has the same form as (38). Thus, for Kuramoto’s model with uniformly distributed natural frequencies $\Omega \in [-\Omega_M, \Omega_M]$, the self-consistent equation (14) for the synchronization onset can be written in the following form:

$$r - r_{\text{lock}} - r_{\text{drift}} = r \left(1 - \frac{\pi}{2} \frac{K}{2\Omega_M} \right) = 0. \tag{39}$$

Summarizing, we have the following sets of self-consistent equations, respectively, for the increasing K case [I] and decreasing K case [II]:

[I] increasing K case: if $\Omega_p < \Omega_M$ ($; K < K_c^{\text{upper}}$), $r = r_{\text{lock}}^I + r_{\text{drift}}^I$, then from (35) and (37)

$$r \left\{ 1 - \frac{K}{2\Omega_M} (\theta_p + \frac{1}{2} \sin 2\theta_p) + \frac{K}{2\Omega_M} \left[-\frac{1}{2} \Delta^2 \right]_{\Omega_p}^{\Omega_M} \right\} = 0; \tag{40}$$

if $\Omega_p \geq \Omega_M$ ($; K > K_c^{\text{upper}}$), $r = r_{\text{lock}}^M \equiv Kr \int_{-\theta_M}^{\theta_M} \cos^2 \theta g(Kr \sin \theta) d\theta = (Kr/2\Omega_M)(\theta_M + \frac{1}{2} \sin 2\theta_M)$ and from (37)

$$r \left\{ 1 - \frac{K}{2\Omega_M} (\theta_p + \frac{1}{2} \sin 2\theta_p) \right\} = 0, \tag{41}$$

where $\theta_M = \sin^{-1}[\Omega_M/(Kr)]$.

[II] decreasing K case: if $\Omega_D < \Omega_M$ ($; K < K_c^{\text{lower}}$), $r = r_{\text{lock}}^{II} + r_{\text{drift}}^{II}$, and from (35) and (38)

$$r \left\{ 1 - \frac{\pi}{2} \frac{K}{2\Omega_M} + \frac{K}{2\Omega_M} \left[-\frac{1}{2} \Delta^2 \right]_{\Omega_D}^{\Omega_M} \right\} = 0; \tag{42}$$

if $\Omega_D \geq \Omega_M$ ($; K > K_c^{\text{lower}}$), $r = r_{\text{lock}}^M$, leading to the same form as (41),

$$r \left\{ 1 - \frac{K}{2\Omega_M} (\theta_M + \frac{1}{2} \sin 2\theta_M) \right\} = 0. \tag{43}$$

3.4. Discontinuous phase transition at the critical point (K_c, r_c)

In (40) and (42), $r = 0$ is just a formal solution since we assumed $r \gg \delta > 0$ in Section 3.3. However, directly from (8) and (15) the incoherent state

$$r(t) \equiv 0 \quad \forall t, \quad \forall K \quad (44)$$

is verified to be a possible (static) state by setting θ_i as follows. For any $\Omega_* \in [-\Omega_M, \Omega_M]$, assume n (≥ 2) oscillators have this natural frequency and their initial state θ_i ($t = 0$) satisfy $\sum \theta_i(0) = 0$, where the summation is taken over the n oscillators with $\Omega = \Omega_*$. This particular configuration of θ_i leads to $r(t) \equiv 0$ and $\dot{\phi} \equiv \text{constant}$ in t for any N . Of course, this situation is too restricted to model nearly incoherent states with certain (small) fluctuations around the above-mentioned completely incoherent state observed in numerical simulations and only shows the existence of the static $r \equiv 0$ solution in the limit of large N . (For a more general configuration, see the discussion in [25].)

On the other hand, for certain large K the coherence r can be determined by (41) or (43). This (K, r) curve can exist for K such that $\Omega_P \geq \Omega_M$ in case [I] and for $\Omega_D \geq \Omega_M$ in case [II], respectively, as shown in Fig. 1(a). The end points of this curve correspond to $\Omega_P = \Omega_M$ for case [I] and $\Omega_D = \Omega_M$ for case [II]. Since r is shown to be an increasing function of K (see Appendix C) and Ω_P and Ω_D are, respectively, given by $\Omega_P = \frac{1}{4}\pi\sqrt{Kr/m}$ and $\Omega_D = Kr$, Ω_P and Ω_D are increasing functions of K . Hence, we can determine these end points $(K_c^{\text{upper}}, r_c^{\text{upper}})$ for [I] and $(K_c^{\text{lower}}, r_c^{\text{lower}})$ for [II] as follows.

For [II]

$$\Omega_M = \Omega_P = (4/\pi)\sqrt{K_c^{\text{upper}}r_c^{\text{upper}}/m} \quad (\text{end point of } (K, r) \text{ curve}), \quad (45)$$

$$1 = \frac{K_c^{\text{upper}}}{2\Omega_M} \left[\theta_P + \frac{1}{2} \sin 2\theta_P \right], \quad (\text{from (41)}) \quad (46)$$

and

$$K_c^{\text{upper}}r_c^{\text{upper}} \sin \theta_P = \Omega_M \quad (\text{from the definition of } \theta_P). \quad (47)$$

For [I]

$$\Omega_M = \Omega_D = K_c^{\text{lower}}r_c^{\text{lower}} \quad (\text{end point of } (K, r) \text{ curve}), \quad (48)$$

$$1 = \frac{\pi K_c^{\text{lower}}}{2\Omega_M} \quad (\text{from (43)}) \quad (49)$$

such that

$$K_c^{\text{lower}} = 4\Omega_M/\pi, \quad r_c^{\text{lower}} = \frac{1}{4}\pi. \quad (50)$$

It should be noted that the above solutions $(K_c^{\text{upper}}, r_c^{\text{upper}})$ and $(K_c^{\text{lower}}, r_c^{\text{lower}})$ lie on the same (K, r) curve defined by the self-consistent equation $r = r_{\text{lock}}$. From (46) and (49), $K_c^{\text{upper}} > K_c^{\text{lower}}$ follows because $\theta_P + \frac{1}{2} \sin 2\theta_P < \frac{1}{2}\pi$ for $0 < \theta_P < \frac{1}{2}\pi$. Since the (K, r) curve is given by a continuous monotonic increasing function $r(K)$ for $K > K_c^{\text{lower}}$ as shown in Appendix C, $r_c^{\text{upper}} > r_c^{\text{lower}} = \frac{1}{4}\pi$ follows.

We now consider the solution of the self-consistent equations if K is below K_c^{lower} for [II] and K_c^{upper} for [I]. We first assume non-zero $r > 0$ exists and show that this cannot be possible; the only possibility is $r = 0$. Given any $r > 0$, the terms $(K/2\Omega_M)[\cdot \cdot \cdot]$ from drifting oscillators in (40) and (42) have some non-zero value and this implies that r is no longer on the coherent (K, r) curve for $K < K_c^{\text{lower}}$ ($/K_c^{\text{upper}}$). From $\Delta \ll 1$ and (32), higher-order

terms in the $(K/2\Omega_M)[\dots]$ term in (40) and (42) are negligibly small and the lowest-order term is dominant. This lowest-order term $(K/2\Omega_M)[-\frac{1}{2}\Delta^2]$ is clearly always positive. For case [II], the $1 - \frac{1}{2}\pi(K/2\Omega_M)$ term in (42) is also positive because $K < K_c^{\text{lower}} = 4\Omega_M/\pi$. Also for [I], the $1 - (K/2\Omega_M)(\theta_p + \frac{1}{2}\sin 2\theta_p)$ term in (40) is shown to be positive for $K < K_c^{\text{upper}}$ from a straightforward calculation (see Appendix C). Thus, both for [I] and [II], the $\{\dots\}$ terms in (40) and (42) are always positive, proving non-existence of any non-zero (static) coherence $r > 0$ for $K < K_c^{\text{upper}}$ and $K < K_c^{\text{lower}}$.

The above reasoning also applies to Kuramoto's model with uniformly distributed natural frequencies, whose self-consistent equation for the synchronization onset is given by (39).

4. Numerical simulations

As we see in (25), in Section 3.3, we do not have to consider m and Ω_M ($/K$) separately. Thus, for numerical simulation purpose we fix the distribution of Ω as $\Omega_M = 5.0$ and gradually change m in a region of large mK .

4.1. Numerical scheme

The numerical simulations of (5) were performed using a fourth-order Runge–Kutta integration scheme with a timestep 0.2. Several of the results were checked with a timestep 0.05. The number of oscillators usually used was 500. In the numerical simulations, we choose N evenly spaced natural frequencies Ω_i on the interval $[-\Omega_M, \Omega_M]$ such that $\Omega_i = -\Omega_M + 2(i-1)\Omega_M/(N-1)$. Two different types of initial conditions are considered: (a) $\theta_i = 0$ and $\omega_i = 0$, and (b) θ_i uniformly distributed in $[0, 2\pi)$ and ω_i also uniformly distributed with $\omega_i = \Omega_i$.

To obtain the (K, r) characteristics, we employed two different schemes (i) and (ii): (i) starting from (b), K is varied up until all oscillators are coherently locked and r becomes $r \simeq 1$, and then K is varied down without feeding new initial condition for θ_i and ω_i from outside; and (ii) in increasing/decreasing K , the initial conditions are given as in (b)/(a), respectively for each update of K . The results are compared for several choices of m and Ω_M , and it is verified that the (K, r) characteristics obtained from (i) and (ii) do not show significant differences except for small fluctuations near the critical K of the coherence onset. Most of the numerical results presented in this section were obtained by scheme (i).

4.2. Critical points and discontinuous jumps

Fig. 4 shows a typical example of the hysteretic synchrony observed numerically. These data were obtained using the scheme (i) for $N = 500$ and $m = 0.85$. As we showed theoretically in Section 3, the discontinuous jumps were observed at two different critical points of (K, r) . From the enlargement of Fig. 4, these critical points are: $(K, r) \simeq (6.37, 0.785)$ and $(K, r) \simeq (13.77, 0.966)$. The theoretical values from (45)–(47) and (50) lead to the corresponding points: $(K, r) \simeq (6.366, 0.785)$ and $(K, r) \simeq (13.44, 0.975)$.

A non-stational oscillation of r was observed when we chose m larger than $m \sim 0.90$. For such m -values and in a range of K the oscillators have a partially coherent, oscillating state from the initial (nearly) incoherent state. As shown in Fig. 5, this oscillating state onsets at a certain K and exists below the critical K above which all the oscillators coherently synchronize. Careful examination of the data from the enlargement of Figs. 5(a)–(c) leads to the numerically obtained upper critical points:

$$\begin{aligned} \text{for } m = 0.90, \quad (K, r) &\simeq (14.61, 0.979), \\ \text{for } m = 0.95, \quad (K, r) &\simeq (15.32, 0.981), \\ \text{for } m = 1.0, \quad (K, r) &\simeq (15.92, 0.982). \end{aligned}$$

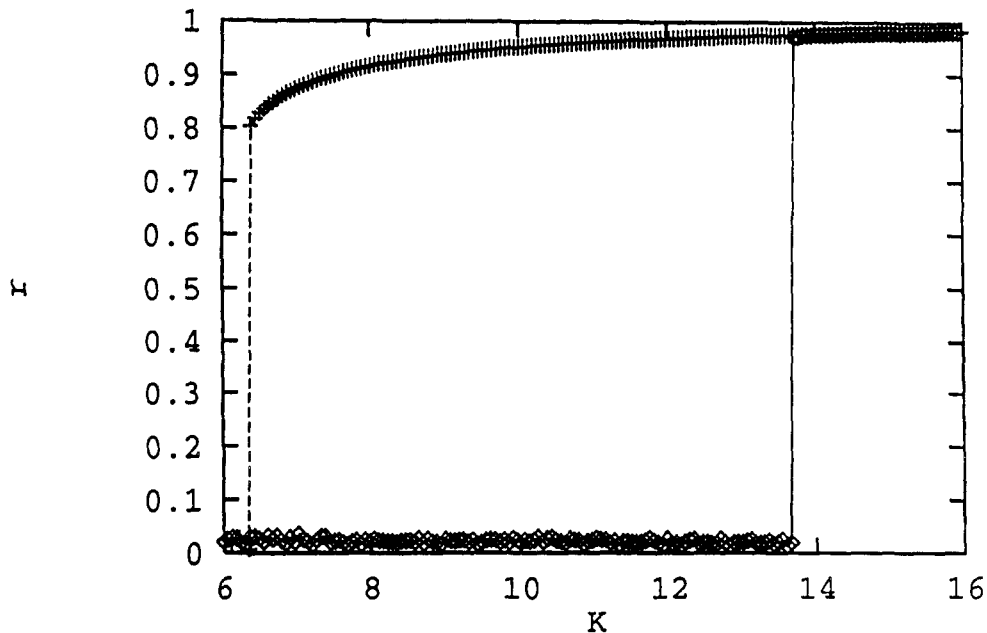


Fig. 4. Typical example of the hysteretic synchrony; $m = 0.85$, $N = 500$ and $\Omega_M = 5.0$.

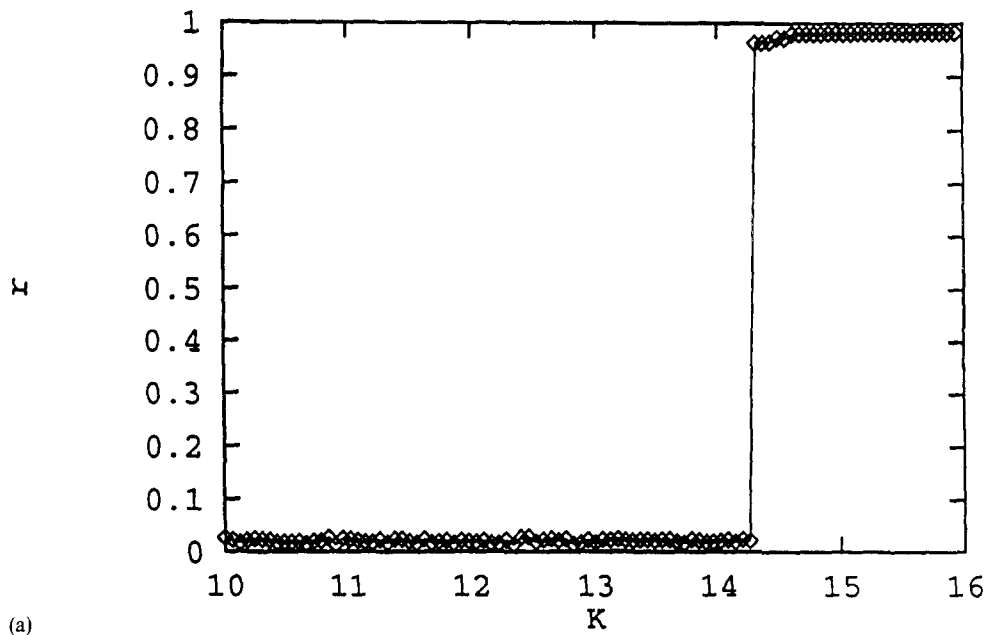


Fig. 5. Incoherent state, oscillating r state, and coherent locked state, observed with increasing coupling strength K : (a) $m = 0.90$; (b) $m = 0.95$; (c) $m = 1.00$.

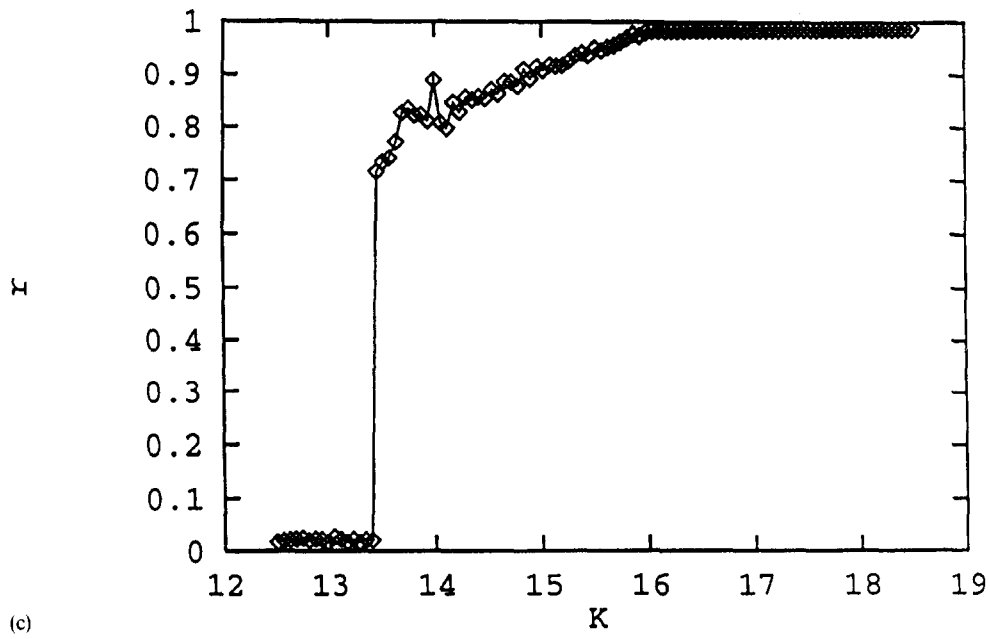
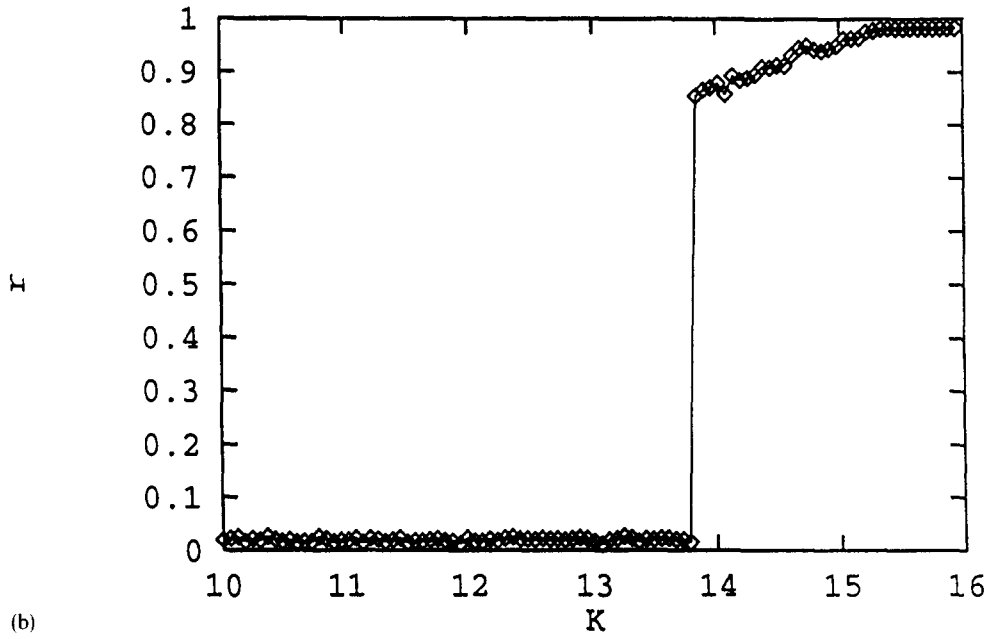


Fig. 5. Continued.

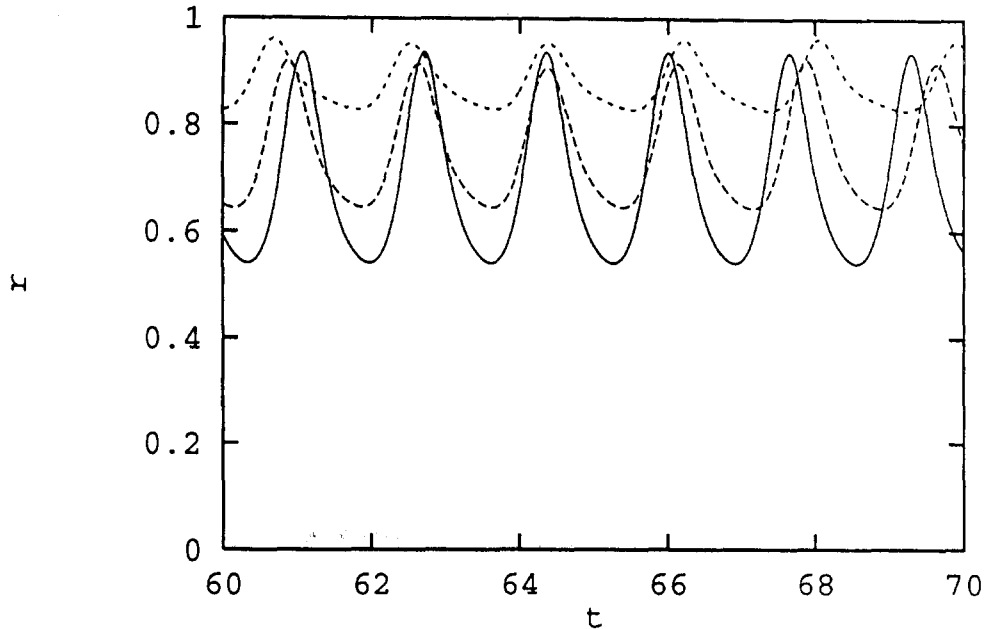


Fig. 6. Wave forms of oscillating r for $m = 0.95$; $K = 12.0$ (solid curve), $K = 13.0$ (dashed curve), and $K = 14.0$ (dotted curve).

Solving (45)–(47) leads to the theoretical values of the upper critical points:

$$\text{for } m = 0.90, \quad (K, r) \simeq (14.19, 0.978),$$

$$\text{for } m = 0.95, \quad (K, r) \simeq (14.95, 0.980),$$

$$\text{for } m = 1.0, \quad (K, r) \simeq (15.70, 0.982).$$

These results, along with the above data for $m = 0.85$, show reasonable agreement between the simulations and the theoretical predictions, and the agreement improves as m becomes larger. Thus, we have verified the existence of the upper critical point $(K_c^{\text{upper}}, r_c^{\text{upper}})$ as obtained from the stationarity assumption [A1] for the coherence r . The oscillating r state, however, clearly breaks the assumption [A1] and therefore cannot be explained from the theory in Section 3.

4.3. Oscillation of r

We now focus our attention on the oscillating state. Wave forms of r are shown in Fig. 6 for $m = 0.95$, $N = 500$, for three values of K , which seem to be periodic. As we see in Figs. 5(a)–(c), the range of K showing an oscillation of r increases as m is increased. More specifically, the oscillating region of K is defined by the region of K values for which there is a spontaneous transition from an incoherent state to an oscillating state (upper critical K_c^{upper}) – (oscillation onset K_{osc}). In Fig. 7, we compare the oscillation onsets for different system size $N = 300, 500$, and 700 using the scheme (i). The result shows the onset K_{osc} is increased as N becomes larger and K_{osc} seems to tend to K_c^{upper} . However, this does not necessarily imply an oscillating state cannot exist, as N gets large, for specific initial conditions. To see if such an oscillation of r can be a possible state for large N , we numerically explore (5) for various N up to 2500, using the following initial conditions: (c) θ_i and ω_i are given as in (b) for $|\omega_i(0)| = |\Omega_i| \geq 0.1$, otherwise $\theta_i(0) = 0$ and $\omega_i(0) = \Omega_i$. As shown in Fig. 8, the amplitude of the

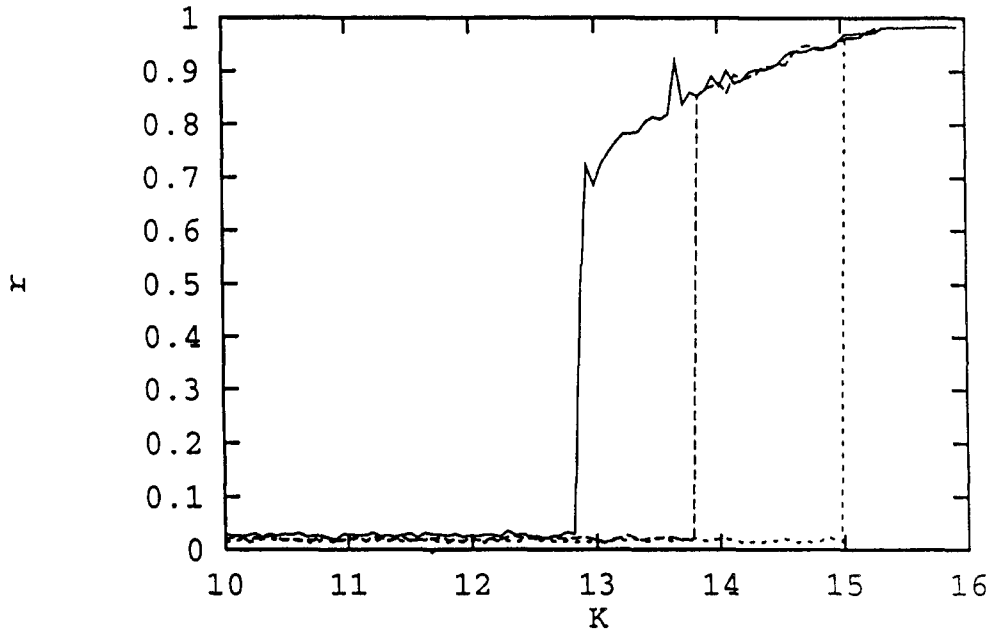


Fig. 7. Oscillation onset for different system sizes N ; $N = 300$ (solid curve), $N = 500$ (dashed curve), $N = 700$ (dotted curve).

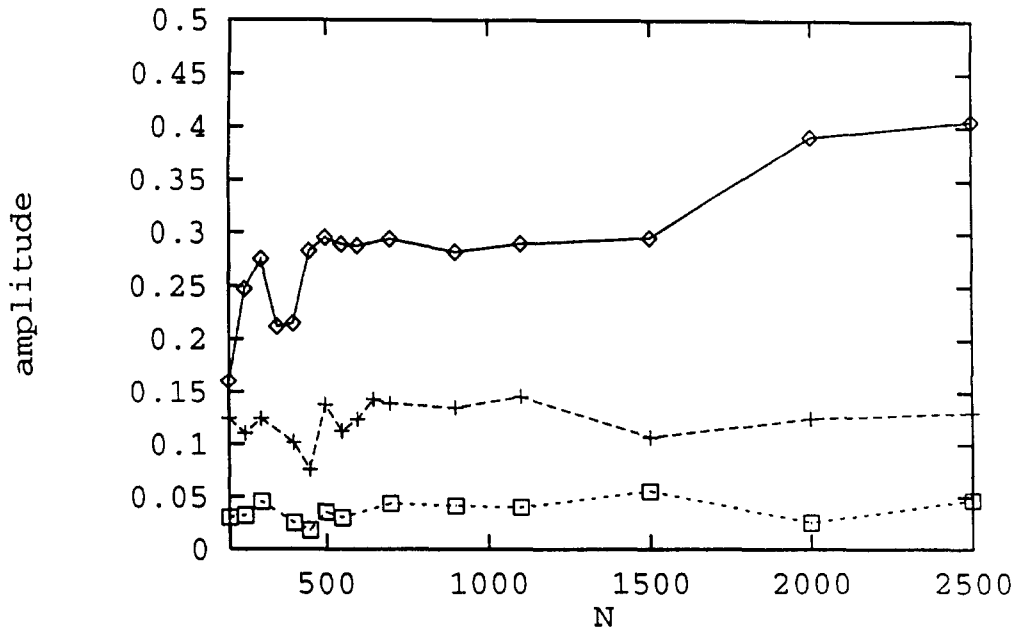


Fig. 8. Oscillation amplitude for different system sizes N with $m = 0.95$, and $K = 12.0$ (\diamond), $K = 13.0$ ($+$) and $K = 14.0$ (\square).

oscillation of r does not decrease as N is increased to 2500. This result, along with the result in Fig. 7, seems to support the following conjecture: an oscillating state can be a possible state in the large N limit for a range of m and K , for certain initial conditions. The transition from the incoherent state to this oscillating state can be triggered by fluctuations in the (nearly) incoherent state, which increase with decreasing N .

5. Conclusion and discussion

In this paper, we studied the collective dynamics of coupled, many oscillator systems with hysteretic characteristics. To facilitate the analysis, we made two assumptions familiar from statistical mechanics: that the coupling between oscillators is global and that the system is infinitely large. These assumptions made it possible to determine the onset of collective synchrony in a self-consistent manner, which can be considered as a higher-order extension of Kuramoto's theory. We have shown that, both for the extended Kuramoto's equation (5), as well as Kuramoto's equation with uniformly distributed natural frequencies, infinitely many oscillators exhibit a discontinuous first-order phase-transition-like change between the incoherent state and the coherent synchronized state. We have also shown that, depending on initial conditions, this transition takes place at different critical values K_c^{lower} and K_c^{upper} . The K_c^{lower} value is the same as Kuramoto's, while the K_c^{upper} value is larger than K_c^{lower} . Our numerical simulations show that an oscillatory r state can exist and bifurcate at $K = K_c^{\text{lower}}$ from the coherent state for non-small m .

Discontinuous jumps have also been found and examined analytically in a CDW model with a global coupling structure [29] and also numerically observed even in randomly coupled neural elements [26]. A common feature of these systems is the existence of a uniformly distributed random variable in a finite interval, e.g. the random pinning in [29] and the uniformly random natural frequencies in [26]. The question naturally arises if the uniform distribution of the random variable is the cause of the discontinuous jumps. Comparison of a uniform distribution with a non-uniform distribution of the natural frequencies in (5) is in progress.

Daido examined the first-order system (1) with matched, general periodic function $H_{ij}(\cdot) \equiv h(\cdot)$ and a Lorentzian distribution $g(\Omega)$. He showed that hysteresis and bistability occurs in the "inverted bifurcation" for certain non-sinusoidal functions [6]. He called this phenomenon *coupling induced* hysteresis and bistability. Even for the Kuramoto model with symmetric and double-peaked distribution $g(\Omega)$, such hysteresis appears [2]. Compared to Daido's work [6], this might be called *frequency distribution induced* hysteresis. While, the hysteresis in the extended Kuramoto model reflects the hysteretic response in each oscillator and therefore might be called *adaptation induced* or *inertia induced* hysteresis, although we only considered a non-generic uniformly distributed frequency distribution in this article.

There are also several mathematical and experimental open problem as follows.

- (1) Although we have verified the oscillating state of r up to $N = 2500$, it is not yet clear how this state can be characterized in the large N limit. Also, if such a state is possible in the large N limit, how can the stability of this state be related to m ?
- (2) We have shown that for a range of K the coherent locked state and the incoherent state can coexist. However, we have not proved these are stable. Also, we have not proved whether the incoherent state is destabilized above $K > K_c^{\text{upper}}$ or not.
- (3) In the synchronous firing of a swarm of the fireflies, the strength of mutual entrainment K can be interpreted as a ratio of the firing brightness to the background brightness. Thus, K should be varied up/down as it gets dark/light in the laboratory experiment. It would be very interesting to observe if a swarm of *P. malaccas* exhibits a hysteresis in its synchrony as it gets dark/light.
- (4) Recent studies on Josephson junction arrays revealed that their synchrony can be hysteretic depending on initial condition when the second-order time derivative ($\beta\ddot{\phi}$) is not negligibly small in the governing equation.

Wiesenfeld pointed out that such a hysteretic synchrony may be related to the hysteresis found in the present study. Can we explain the hysteresis in Josephson junction arrays in such a self-consistent theory? Work in this direction is in progress.

Acknowledgements

One of the authors (HT) deeply thanks Prof. M.A. Lieberman and Dr. M. de Sousa Vieira for their continuous support and helpful discussions. He would like to thank Dr. S. Watanabe (Niels Bohr Institute) for many stimulating discussions over the year and Prof. K. Wiesenfeld for his comments on the applications to the Josephson junction arrays. Thanks are also due to Prof. S.H. Strogatz for fruitful discussions on the second-order phase model and Kuramoto's theory at the Jackson Hole meeting. HT also thanks Prof. T. Endo (Meiji University) and Prof. R. Hirota (Waseda University) for their helpful comments and encouragements. This work was initiated at the 1995 IIAS summer seminar organized by Prof. A. Hasegawa and Prof. N. Itoh. HT thanks Professors N. Itoh, K. Gohara, M. Kikuchi, H. Nishimori, T. Ohira, T. Yanagita and H. Yuasa, and other participants for their helpful discussions. The research of HT, was supported in part by JSPS Research Fellowships for Young Scientists.

Appendix A. Approximation of the $\cos \theta$ term

This appendix gives a calculation for the $\cos \theta$ term needed in Section 3.4. We employed the approximation of θ : $\theta(\tau) = \theta_0 + \delta^2 \theta_2 + \delta^3 \theta_3$, discarding δ^n ($n \geq 4$) terms. This yields a good approximation of $\cos \theta(\tau)$ because $\delta^4 (K/\Omega)^4 \tilde{r}^2 = (\Delta^4 \tilde{r})^2$ becomes small compared to the coefficients in the lower-order terms. Then, $\cos \theta(\tau)$ can be expressed by the Bessel functions as follows:

$$\begin{aligned} \cos \theta(\tau) &\simeq \cos[\tau + \Delta^2 \tilde{r} \sin \tau + \Delta^3 \tilde{r} \cos \tau - \Delta^3 \tilde{r}] = \cos[\tilde{\Omega} t + a \sin(\tilde{\Omega} t + C + \Delta^3 \tilde{r})] \\ &= J_0(a) \cos \tilde{\Omega} t - J_1(a) \cos(C + \Delta^3 \tilde{r}) + J_1(a) \cos(2\tilde{\Omega} t + C + \Delta^3 \tilde{r}), \\ &\quad + \text{(higher harmonics)} \end{aligned} \quad (\text{A.1})$$

leading to

$$\int_0^{\tilde{r}} \cos \theta(t) dt = -2(\pi/\tilde{\Omega}) J_1(a) \cos(C + \Delta^3 \tilde{r}), \quad (\text{A.2})$$

where $\Delta = (m\Omega)^{-1}$, and a and C are determined from

$$\begin{aligned} a \sin(\tau + C) &= \Delta^2 \tilde{r} \sin \tau + \Delta^3 \tilde{r} \cos \tau, \\ a &= \Delta^2 \sqrt{1 + \Delta^2 \tilde{r}}, \quad \sin C = 1/\sqrt{1 + \Delta^2}, \quad \cos C = \Delta/\sqrt{1 + \Delta^2}. \end{aligned} \quad (\text{A.3})$$

If $\Delta \ll 1$, (A.2) can be further approximated as follows. In Section 3.3, we obtained $J_1(a) \simeq \frac{1}{2}a = \Delta^2 \sqrt{1 + \Delta^2} \cdot \tilde{r}/2$. Using this approximation and (A.3), the $J_1(a) \cos(C + \Delta^3 \tilde{r})$ term in (33) can be given as

$$\begin{aligned} J_1(a) \cos(C + \Delta^3 \tilde{r}) &\simeq \frac{1}{2} \tilde{r} \Delta^2 \sqrt{1 + \Delta^2} [\cos(\Delta^3 \tilde{r})(\Delta/\sqrt{1 + \Delta^2}) - \sin(\Delta^3 \tilde{r})(1/\sqrt{1 + \Delta^2})] \\ &= \frac{1}{2} \tilde{r} [\Delta^3 \cos(\Delta^3 \tilde{r}) - \Delta^2 \sin(\Delta^2 \tilde{r})] \end{aligned} \quad (\text{A.4})$$

As $\Delta \leq (m\Omega_P)^{-1} = (4/\pi)\sqrt{(\delta/r)} \ll 1$ (see Appendix B) and $\Delta^3\bar{r} = \Delta^2\bar{r} \cdot \Delta \ll 1$, $\cos(\Delta^3\bar{r}) \simeq 1 - \frac{1}{2}(\Delta^3\bar{r})^2 + O([\Delta^3\bar{r}]^4)$ and $\sin(\Delta^3\bar{r}) \simeq \Delta^3\bar{r} + O([\Delta^3\bar{r}]^3)$ follow. Neglecting $O([\Delta^3\bar{r}]^4)$ terms in the cos term and $O([\Delta^3\bar{r}]^3)$ terms in the sin term, we finally obtain the following from (A.4):

$$J_1(a) \cos(C + \Delta^3\bar{r}) \simeq \frac{1}{2}\bar{r}[\Delta^3 - \bar{r}\Delta^5 - \frac{1}{2}\bar{r}^2\Delta^9]. \quad (\text{A.5})$$

Appendix B. Analytic expression of Ω_P

This appendix gives an analytic expression of Ω_P needed in Section 3.4. A new time-scale $t_{\text{new}} = \sqrt{(Kr/m)}t_{\text{old}}$ transforms (15) to the following form:

$$\ddot{\theta} + (1/\sqrt{mKr}) \cdot \dot{\theta} + \sin \theta = \Omega/(Kr). \quad (\text{B.1})$$

Using $1/\sqrt{mKr} = \delta(\sqrt{\bar{r}}/r)$ and $\Omega/(Kr) = \delta(\Omega m/r)$, (B.1) becomes

$$\ddot{\theta} = -\sin \theta + \delta(m\Omega/r - (\sqrt{\bar{r}}/r)\dot{\theta}) \equiv -\sin \theta + \delta(I - \alpha\dot{\theta}). \quad (\text{B.2})$$

Eq. (B.2) has a suitable form for Melnikov's analysis, if $\delta \ll 1$, $I \equiv \Omega m/r = O(1)$ and $\alpha \equiv \sqrt{\bar{r}}/r = O(1)$. The homoclinic bifurcation curve in the (I, α) parameter space is tangent to the line $I = 4\alpha/\pi$ and this line is close to the homoclinic bifurcation curve even if $\delta\alpha$ is not so small (see [10,28]). Thus, we obtain the approximation of Ω_P from $I = 4\alpha/\pi$, i.e. $m\Omega_P/r = (4/\pi)\sqrt{\bar{r}}/r$. The result is given as

$$\Omega_P = \frac{4}{\pi} \sqrt{\frac{Kr}{m}}. \quad (\text{B.3})$$

Appendix C. K, r curve defined by $r = \mathcal{D} r_{\text{lock}}$

This appendix gives an analytic expression for the (K, r) curve for $K > K_c^{\text{lower}}$, which is defined by (41) or (43). We prove here $K = K(r)$ is a continuous monotonic increasing function of r . Eliminating K from (43) and setting $\sin \theta_P = \Omega_M/(Kr)$, we obtain

$$r(\theta_P) = \frac{\theta_P + (1/2) \sin 2\theta_P}{2 \sin \theta_P}. \quad (\text{C.1})$$

Then, $r'(\theta_P)$ becomes

$$r'(\theta_P) = \frac{\cos \theta_P}{2 \sin^2 \theta_P} \left(\frac{1}{2} \sin 2\theta_P - \theta_P \right), \quad (\text{C.2})$$

which is always negative for $0 < \theta_P < \frac{1}{2}\pi$. Hence, $r(\theta_P)$ is a monotone decreasing function of θ_P . Also, (43) shows that $K(\theta_P)$ is a monotone decreasing function of θ_P . Thus, $r(K)$ is a monotone increasing function of K . The continuity of $r(K)$ is clear from (43) and $\sin \theta_P = \Omega_M/(Kr)$.

We show below that the $1 - (K/2\Omega_M)(\theta_P + \frac{1}{2} \sin 2\theta_P)$ term in (40) is positive. By letting $K(\theta_P + \frac{1}{2} \sin 2\theta_P) \equiv f(K)$,

$$\frac{df(K)}{dK} = (\theta_P + \frac{1}{2} \sin 2\theta_P) + K(1 + \cos 2\theta_P) \frac{d\theta_P}{dK} \quad (\text{C.3})$$

follows. From $\sin \theta_P = \Omega_P/(Kr) = (4/\pi)(mrK)^{-1/2}$, the following relations are obtained:

$$\frac{1}{2} \sin 2\theta_P = (4/\pi)^2 (mrK)^{-1/2} \left[\left(\frac{1}{4}\pi \right)^2 - (mrK)^{-1} \right]^{-1/2}, \quad \cos 2\theta_P = 1 - 2(4/\pi)^2 (mrK)^{-1},$$

and

$$\frac{d\theta_p}{dK} = -\frac{1}{2}(mr)^{-1/2}K^{-2/3}\left[\left(\frac{1}{4}\pi\right)^2 - (mrK)^{-1}\right]^{-1/2}.$$

Using these in (C.3), $df(K)/dK$ can be simplified to $df(K)/dK = \theta_p > 0$. As $1 - (K/2\Omega_M)(\theta_p + \frac{1}{2}\sin 2\theta_p) = 0$ for $K = K_c^{\text{lower}}$ and $df(K)/dK > 0$, $1 - (K/2\Omega_M)(\theta_p + \frac{1}{2}\sin 2\theta_p) > 0$ for $K < K_c^{\text{lower}}$ follows.

References

- [1] Y. Aizawa, Synergetic approach to the phenomena of mode-locking in nonlinear systems, *Prog. Theoret. Phys.* 56 (1976) 703–716.
- [2] L.L. Bonilla, J.C. Neu and R. Spigler, *J. Stat. Phys.* 67 (1992) 313.
- [3] J.D. Crawford, Scaling and singularities in the entrainment of globally coupled oscillators, *Phys. Rev. Lett.* 74 (1995) 4341–4344.
- [4] F. Crick and C. Koch, Toward a neurobiological theory of consciousness, *Seminars Neurosci.* 2 (1990) 263–275.
- [5] H. Daido, Lower critical dimension for populations of oscillators with randomly distributed frequencies: A renormalization group analysis, *Phys. Rev. Lett.* 61 (1988) 231–234.
- [6] H. Daido, Onset of cooperative entrainment in limit-cycle oscillators with uniform all-to-all interactions: Bifurcation of the order function, *Physica D* 91 (1996) 24–66.
- [7] M. de Sousa Vieira, A.J. Lichtenberg and M.A. Lieberman, Self-synchronization of many coupled oscillators, *Int. J. Bifurcation Chaos* 4 (1994) 1563–1577.
- [8] G.B. Ermentrout, An adaptive model for synchrony in the firefly *Pteroptyx malaccae*, *J. Math. Biol.* 29 (1991) 571–585.
- [9] C.M. Gray, P. König, A.K. Engel and W. Singer, Oscillatory responses in cat visual cortex exhibit inter-columnar synchronization which reflect global stimulus properties, *Nature* 338 (1989) 334–337.
- [10] J. Guckenheimer and P. Holmes, *Nonlinear Oscillations, Dynamical Systems, and Bifurcations of Vector Fields* (Springer, New York, 1983).
- [11] P. Hadley and M.R. Beasley, Dynamical states and stability of linear arrays of Josephson junctions, *J. Appl. Phys.* 50 (1987) 621–623.
- [12] F.E. Hanson, Pacemaker control of rhythmic flashing of fireflies, in: *Cellular Pacemakers*, ed. D.O. Carpenter, Vol. 2 (Wiley, New York, 1982) pp. 81–100.
- [13] J.J. Hopfield, Pattern recognition computation using action potential timing for stimulus representation, *Nature* 376 (1995) 33–36.
- [14] T. Konishi and K. Kaneko, Clustered motion in symplectic coupled map systems, *J. Phys. A.* 25 (1992) 6283–6296.
- [15] Y. Kuramoto, Self-entrainment of a population of coupled nonlinear oscillators, in: *Int. Symp. on Mathematical Problems in Theoretical Physics*, ed. H. Araki, *Lecture Notes in Physics*, Vol. 39 (Springer, New York, 1975) pp. 420–422.
- [16] Y. Kuramoto, *Chemical Oscillation, Waves and Turbulence* (Springer, Berlin, 1984).
- [17] G. Laurent and H. Davidowitz, Encoding of olfactory information with oscillating neural assemblies, *Science* 265 (1994) 1872–1875.
- [18] M. Levi, F.C. Hoppensteadt and W.L. Miranker, Dynamics of the Josephson junction, *Quart. Appl. Math.* (1978) 167–198.
- [19] A.J. Lichtenberg and M.A. Lieberman, *Regular and Chaotic Dynamics*, 2nd Ed. (Springer, New York, 1992).
- [20] P.C. Matthews, R.E. Mirollo and S.H. Strogatz, Dynamics of a large system of coupled nonlinear oscillators, *Physica D* 52 (1991) 293–331.
- [21] R.E. Mirollo and S.H. Strogatz, Synchronization of pulse-coupled biological oscillators, *SIAM J. Appl. Math.* 50 (1990) 1645–1662.
- [22] N. Nakagawa and Y. Kuramoto, From collective oscillations to collective chaos in a globally coupled oscillator systems, *Physica D* 75 (1994) 74–80.
- [23] E. Niebur, H.G. Schuster, D.M. Kammem and C. Koch, Oscillator-phase coupling from different two-dimensional network connectivities, *Phys. Rev. A* 44 (1991) 6895–6904.
- [24] H. Sakaguchi and Y. Kuramoto, A soluble active rotator model showing phase transitions via mutual entrainment, *Prog. Theoret. Phys.* 76 (1986) 576–581.
- [25] F.M.A. Salam, J.E. Marsden and P.P. Varaiya, Arnold diffusion in the swing equations of a power system, *IEEE Trans. CAS* 32 (1983) 784–796.
- [26] K. Satoh, Computer experiment on the cooperative behaviour of a network of interacting nonlinear oscillators, *J. Phys. Soc. Japan* 58 (1989) 2010–2021.
- [27] S.H. Strogatz, Norbert Wiener's brain waves, in: *Lecture Notes in Biomathematics*, Vol. 100 (Springer, Berlin, 1994).
- [28] S.H. Strogatz, *Nonlinear Dynamics and Chaos* (Addison-Wesley, Reading, MA, 1994) p. 273.
- [29] S.H. Strogatz, C.M. Marcus, R.E. Mirollo and R.M. Westervelt, Collective dynamics of coupled oscillators with random pinning, *Physica D* 36 (1989) 23–50.
- [30] S.H. Strogatz and R.E. Mirollo, Phase-locking and critical phenomena in lattices of coupled nonlinear oscillators with random intrinsic frequencies, *Physica D* 31 (1988) 143–168.
- [31] S.H. Strogatz and R.E. Mirollo, Stability of incoherence in a population of coupled oscillators, *J. Stat. Phys.* 63 (1991) 613–635.

- [32] S. Watanabe and S.H. Strogatz, Constants of motion for superconducting Josephson array, *Physica D* 73 (1994) 197–253.
- [33] S. Watanabe and J.W. Swift, Stability of periodic solutions in series arrays of Josephson junctions with internal capacitance, *J. Nonlin. Sci.*, to appear.
- [34] C.E. Wayne, Bounds on the trajectories of a system of weakly coupled rotators, *Commun. Math. Phys.* 104 (1986) 21–36.
- [35] K. Wiesenfeld, P. Colet and S.H. Strogatz, Synchronization transitions in a disordered Josephson series array, *Phys. Rev. Lett.* 76 (1996) 404–407.
- [36] A.T. Winfree, Biological rhythms and the behavior of populations of coupled oscillators, *J. Theor. Biol.* 16 (1967) 15–42.
- [37] A.T. Winfree, *The Geometry of Biological Time* (Springer, New York, 1980).
- [38] Y. Yamaguchi and H. Shimizu, Theory of self-synchronization in the presence of native frequency distribution and external noises, *Physica D* 11 (1984) 212–226.
- [39] R.A. York and R.C. Compton, Quasi-optical power combining using mutually synchronized oscillator arrays, *IEEE Trans. Microwave Theor. and Tech.* 39 (1991) 1000–1009.